

Copper Hydroxydiphosphate with a One-Dimensional Arrangement of Copper Polyhedra: $\text{Cu}_3[\text{P}_2\text{O}_6\text{OH}]_2$

Radu Baies, Vincent Caignaert,* Valerie Pralong, and Bernard Raveau

Laboratoire CRISMAT, UMR 6508 CNRS ENSICAEN, 6 bd Maréchal Juin, 14050 CAEN Cedex, France

Received October 21, 2004

A new copper hydroxydiphosphate $\text{Cu}_3(\text{P}_2\text{O}_6\text{OH})_2$ was synthesized, by soft chemistry. The crystal structure was solved ab initio from X-ray powder diffraction data in the triclinic space group $P\bar{1}$. The structure is built up from $[\text{Cu}_3\text{O}_{10}]_\infty$ zigzag chains linked by $\text{P}_2\text{O}_6(\text{OH})$ groups to form a tridimensional framework. The $[\text{Cu}_3\text{O}_{10}]_\infty$ chains consist of edge-sharing polyhedra. The structure contains two sorts of copper polyhedra: one CuO_6 octahedron and two CuO_5 pyramids. Magnetization measurements confirm the presence of divalent copper and suggest antiferromagnetic interactions at low temperature.

Introduction

The numerous investigations of the systems $\text{Cu}-\text{P}-\text{O}$ and $\text{Cu}-\text{P}-\text{O}-\text{H}$ have shown their very rich crystal chemistry. The latter originates from the ability of copper to accommodate various coordinations from tetrahedral or square to pyramidal and octahedral, whereas phosphate groups can also appear with different configurations, i.e., as single PO_4 tetrahedra in monophosphates, as double P_2O_7 groups in diphosphates, as rings in cyclophosphates, or as 3D frameworks in ultraphosphates. Thirteen different structures of copper phosphates or hydroxyphosphates have been discovered to date. The larger family is that of copper monophosphates, which is obtained for molar ratio $\text{Cu}/\text{P} \geq 1$. The latter contain generally two kinds of copper polyhedra in the same structure as shown for $\text{Cu}_2\text{PO}_4(\text{OH})$,¹ $\text{Cu}_3(\text{PO}_4)_2$,² $\text{Cu}_3(\text{PO}_4)_2 \cdot \text{H}_2\text{O}$,³ $\text{Cu}_3\text{PO}_4(\text{OH})_3$,⁴ $\text{HCuPO}_4 \cdot \text{H}_2\text{O}$,⁵ and $\text{Cu}_5(\text{PO}_4)_2(\text{OH})_4$.⁶ More rarely, three different kinds of copper polyhedra may coexist in the same structure as shown for the monophosphates $\text{Cu}_5\text{O}_2(\text{PO}_4)_2$,⁷ $\text{Cu}_5(\text{PO}_4)_2(\text{OH})_4$,⁸ $\text{Cu}_4\text{O}(\text{PO}_4)_2$,⁹ and

$\text{Cu}_9\text{O}_2(\text{PO}_4)_4(\text{OH})_2$.¹⁰ In contrast, polyphosphates are much less numerous. They are synthesized for molar ratio $\text{Cu}/\text{P} \leq 1$. Only one diphosphate $\text{Cu}_2\text{P}_2\text{O}_7$ ¹¹ has been synthesized to date, corresponding to $\text{Cu}/\text{P} = 1$, whereas for $\text{Cu}/\text{P} < 1$, one cyclotetraphosphate $\text{Cu}_2\text{P}_4\text{O}_{12}$ ¹² and one ultraphosphate $\text{Cu}_2\text{P}_8\text{O}_{22}$ ¹³ are actually known.

The extraordinary richness of the crystal chemistry of these copper phosphates for molar ratio $\text{Cu}/\text{P} > 1$, compared to the domain $\text{Cu}/\text{P} < 1$, suggests that the phosphate rich region has not yet been sufficiently explored and that new frameworks remain to be discovered. We have thus revisited the system $\text{Cu}-\text{P}-\text{O}-(\text{H})$, for Cu/P ratios < 1 , using soft chemistry methods in aqueous solution. We report herein on a novel copper hydroxydiphosphate, $\text{Cu}_3[\text{P}_2\text{O}_6\text{OH}]_2$, with an original structure built up of infinite chains of edge-sharing CuO_6 octahedra and CuO_5 pyramids, interconnected with diphosphate groups $\text{P}_2\text{O}_6(\text{OH})$. Magnetic measurements confirm the presence of divalent copper and suggest antiferromagnetic interactions at low temperature.

Experimental Section

Materials and Methods. The chemical were purchased from commercial sources and used as received. The magnetic susceptibility of a powdered sample was measured from 5 to 400 K with a

* To whom correspondence should be addressed. E-mail: vincent.caignaert@ensicaen.fr.

- (1) Heritsch, H. Z. *Kristallogr.* **1940**, *1*, 102.
- (2) Shoemaker, G. L.; Anderson, J. B.; Kostiner, E. *Acta Crystallogr. B* **1977**, *33*, 2969.
- (3) Durif, A.; Guitel, J. C. *J. Solid State Chem.* **1978**, *25*, 39.
- (4) Anderson, J. B.; Shoemaker, G. L.; Kostiner, E. *J. Solid State Chem.* **1978**, *25*, 49.
- (5) Fehlmann, M.; Ghose, S.; Finney, J. J. *J. Chem. Phys.* **1964**, *41*, 1910.
- (6) Boudjada, A. *Mater. Res. Bull.* **1980**, *15*, 1083.
- (7) Anderson, J. B.; Shoemaker, G. L.; Kostiner, E.; Ruzsala, F. A. *Am. Mineral.* **1977**, *62*, 115.
- (8) Brunel-Lauegt, M.; Guitel, J. C. *Acta Crystallogr. B* **1977**, *33*, 3465.
- (9) Ghose, R. *Naturwissenschaften* **1962**, *49*, 324.

- (9) Effenberger, H. *J. Solid State Chem.* **1985**, *57*, 240.
- (10) Yamashita, A.; Kawahara, A. *Acta Crystallogr. C* **1995**, *51*, 1483.
- (11) Lukaszewicz, K. *Bull. Pol. Acad. Sci., Sci. Chem.* **1966**, *14*, 725.
- (12) Robertson, B. E.; Calvo, V. *Acta Crystallogr.* **1967**, *22*, 665.
- (13) Laugt, M.; Guitel, J. C.; Tordjman, I.; Bassi, G. *Acta Crystallogr. B* **1972**, *28*, 201.
- (14) Olbertz, A.; Stachel, D.; Svoboda, I.; Fuess, H. *Z. Kristallogr.* **1996**, *211*, 551.

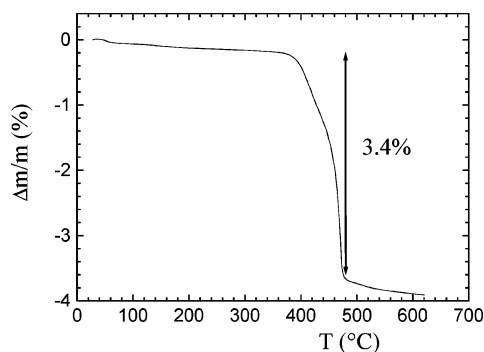


Figure 1. TGA curve for dehydration of $\text{Cu}_3(\text{P}_2\text{O}_6\text{OH})_2$ under argon.

SQUID magnetometer (MPMS, Quantum Design) for an applied field $\mathbf{B} = 3000$ Oe. The sample was first zero field cooled at 5 K until stable temperature before applying the magnetic field. The infrared (IR) spectrum was recorded in the range $500\text{--}2000\text{ cm}^{-1}$ by means of a Nicolet Nexus spectrometer. Measurements involving the coaddition of 32 scans with a nominal resolution of 5 cm^{-1} were performed on samples diluted in powdered KBr (1%); the spectrum of pure KBr was subtracted from the sample spectrum. Thermogravimetric studies were carried out with a Setaram TG 92 instrument at a heating rate of $1\text{ }^\circ\text{C}/\text{min}$ under flowing argon gas. A scanning electron microscope (SEM) Philips Field Effect Gun (FEG) XL-30 with a resolution of about 1 nm was used to study the sample morphology, while elemental compositions were determined by energy dispersive spectroscopy (EDS) on a Link-Isis analyzer (ATW 6650 detector).

Synthesis. The compound was prepared by heating a mixture of 0.5 g of CuO and 20 mL of H_3PO_4 at $152\text{ }^\circ\text{C}$ in a Teflon beaker under continuous stirring. The beaker was put in a thermostated oil bath and kept in the above condition for 24 h. Named compound appeared as light blue powder which decanted easily in a few minutes when the stirrer was stopped. The solution was cooled to room temperature, and the phosphoric acid was dropped out. The product was first washed with distilled water and then with pure acetone for a few times, to remove the phosphoric acid. The X-ray pattern of this phase revealed a similarity to the phase $\text{CuH}_2\text{P}_2\text{O}_7$, reported in the JCPDS-ICDD database [PDF no. 340605], without matching perfectly. The synthesis of $\text{CuH}_2\text{P}_2\text{O}_7$ ¹⁴ appears rather similar to the one we used. The average molar ratio between copper and phosphorus P/Cu, determined by EDS, was found to be close to 1.4, i.e., lower than expected for $\text{CuH}_2\text{P}_2\text{O}_7$. Moreover the loss of water (3.4% in weight between 350 and $500\text{ }^\circ\text{C}$), determined by thermogravimetric analysis (TGA) (Figure 1), suggested the chemical composition $\text{Cu}_3\text{H}_2\text{P}_4\text{O}_{14}$ (loss of water, 3.33% in weight). This composition was confirmed later by the crystallographic study.

Structure Solution and Refinement. The structure solution was performed using a conventional high-resolution Seifert 3000 diffractometer with $\lambda\text{ CuK}\alpha_1$ radiation. The X-ray pattern was registered between 10° and 80° (2θ) with a step of 0.02° at room temperature. The first 20 reflections were indexed using the auto-indexing software TREOR.¹⁵ The program gave a triclinic solution with a figure of merit $M(20) = 47$.¹⁶ The cell parameters were $a = 4.782\text{ \AA}$, $b = 7.037\text{ \AA}$, $c = 8.357\text{ \AA}$, $\alpha = 66.68^\circ$, $\beta = 76.99^\circ$, and $\gamma = 72.06^\circ$. The EXPO¹⁷ package, integrating SIR97¹⁸ for direct methods structure solution, was used to solve the structure in the

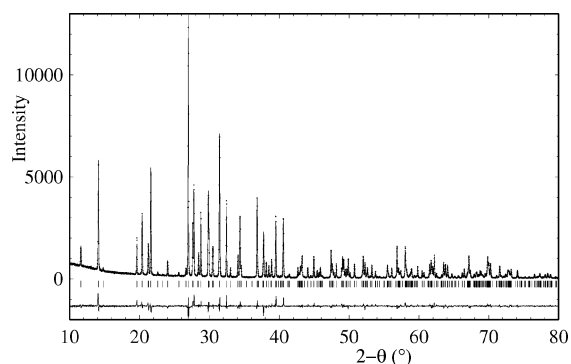


Figure 2. Rietveld refinement plot of X-ray diffraction data for $\text{Cu}_3(\text{P}_2\text{O}_6\text{OH})_2$. Observed, calculated, and difference profiles are plotted on the same scale. The Bragg peaks are indicated by tick marks.

Table 1. Crystallographic Data for $\text{Cu}_3(\text{P}_2\text{O}_6\text{OH})_2$

formula	$\text{Cu}_3\text{H}_2\text{O}_{14}\text{P}_4$
fw	540.54
space group	$P\bar{1}$
a , \AA	4.78191(6)
b , \AA	7.03699(8)
c , \AA	8.35740(8)
α , deg	66.6790(6)
β , deg	76.9930(7)
γ , deg	72.0642(6)
V , \AA^3	243.983(4)
Z	1
ρ_{calc} , g/cm^3	3.679
R_{wp}	0.0957
R_{p}	0.0728
R_{B}	0.0585

$P\bar{1}$ space group. The second best solution computed by SIRPOW gave positions of all non-hydrogen atoms. This structural model was used as a starting model for Rietveld refinement using FullProf.¹⁹ The refinement of the 30 atomic coordinates and one overall thermal factor converged to satisfactory agreement factors ($R_{\text{WP}} = 13.9\%$, $R_{\text{B}} = 7.16\%$, and $\chi^2 = 3.86$). Although interatomic distances are not as accurate as with single crystal data, no restraints on distances were necessary to obtain a chemically reasonable structure. The last cycle of refinement conducted with 47 variable parameters (30 atomic parameters, 3 thermal parameters, 6 cell parameters, 7 profile parameters, and 1 scale factor) converged with the following agreement factors: $R_{\text{WP}} = 9.57\%$, $R_{\text{B}} = 5.85\%$, and $\chi^2 = 3.17$. The final Rietveld refinement plot is given in Figure 2. A summary of crystallographic data is given in Table 1. The crystallographic parameters are presented in Table 2.

Results and Discussion

Structure of $\text{Cu}_3(\text{P}_2\text{O}_6\text{OH})_2$. The projection of the structure along \vec{a} (Figure 3) shows that the tridimensional “ $\text{Cu}_3\text{P}_4\text{O}_{14}$ ” framework consists of diphosphate P_2O_7 groups, $\text{Cu}(1)\text{O}_6$ octahedra, and $\text{Cu}(2)\text{O}_5$ pyramids, forming rectangular and diamond shaped tunnels running along \vec{a} . The P_2O_7 groups are isolated from each other, each group sharing five apexes with copper polyhedra, whereas copper polyhedra

(14) Lavrov, A. V.; Bykanova, T. A.; Tezikova, L. A. *Inorg. Mater.* **1975**, *11*, 771.

(15) Werner, P.-E.; Eriksson, L.; Westdahl, M. *J. Appl. Crystallogr.* **1985**, *18*, 367.

(16) Wolff, P. M. *J. Appl. Crystallogr.* **1968**, *1*, 108.

(17) Altomare, A.; Burla, M. C.; Camilli, M.; Carrozzini, B.; Cascarano, G. L.; Giacovazzo, C.; Guagliardi, A.; Moliterni, A. G. G.; Polidori, G.; Rizzi, R. *J. Appl. Crystallogr.* **1999**, *32*, 339.

(18) Altomare, A.; Burla, M. C.; Cascarano, G. L.; Giacovazzo, C.; Guagliardi, A.; Moliterni, A. G. G.; Polidori, G. *J. Appl. Crystallogr.* **1995**, *28*, 842.

(19) Rodriguez-Carvajal, J. *Collected Abstracts of Powder Diffraction Meeting, Toulouse, France, 1990*; p 127.

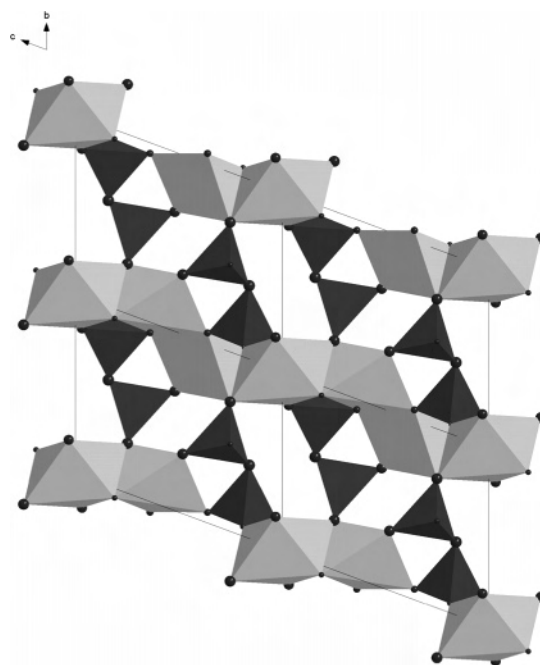
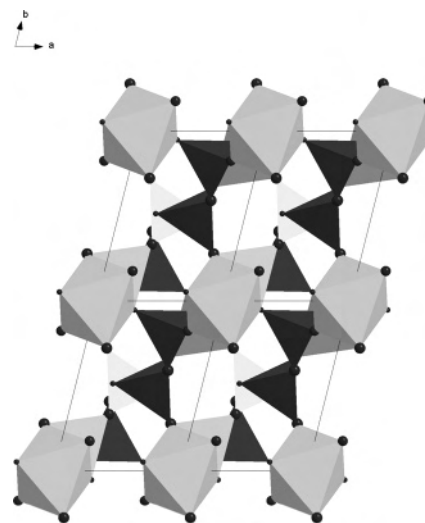
Table 2. Fractional Atomic Coordinates and Isotropic Thermal Factors for $\text{Cu}_3(\text{P}_2\text{O}_6\text{OH})_2$

atom	x	y	z	B (\AA^2)
Cu1	0	0	0	0.38(8)
Cu2	0.9441(8)	0.8471(6)	0.4288(5)	0.38(8)
P3	0.6310(14)	0.5070(11)	0.7031(9)	0.29(12)
P4	0.6458(15)	0.8439(10)	0.8121(9)	0.29(12)
O5	0.681(3)	0.6641(19)	0.5197(17)	0.77(16)
O6	0.819(3)	0.9407(19)	0.6343(17)	0.77(16)
O7	0.287(3)	0.515(2)	0.7488(16)	0.77(16)
O8	0.698(3)	0.595(2)	0.8382(16)	0.77(16)
O9	0.782(3)	0.8245(19)	0.9679(17)	0.77(16)
O10	0.175(3)	0.718(2)	0.2555(16)	0.77(16)
O11	0.317(3)	0.944(2)	0.8123(16)	0.77(16)

share their edges forming $[\text{Cu}_3\text{O}_{10}]_\infty$ chains running along \vec{c} . The P_2O_7 groups and the $[\text{Cu}_3\text{O}_{10}]_\infty$ chains are displayed in layers parallel to the (\vec{a}, \vec{c}) plane. One plane of P_2O_7 groups alternates with one plane of $[\text{Cu}_3\text{O}_{10}]_\infty$ chains. In each chain one CuO_6 octahedron alternates with two CuO_5 tetragonal pyramids along \vec{c} , the apical apexes of the two edge-shared pyramids being in trans positions with respect to each other. This chain forms a one-dimensional “zigzag” chain built up with linear trimers $\text{Cu}(2)-\text{Cu}(1)-\text{Cu}(2)$. The $\text{Cu}(1)\text{O}_6$ octahedron shares trans edges with two $\text{Cu}(2)\text{O}_5$ pyramids, while the $\text{Cu}(2)\text{O}_5$ pyramid shares cis and trans edges with neighboring $\text{Cu}(1)\text{O}_5$ and $\text{Cu}(2)\text{O}_6$ polyhedra. Similar chains, exclusively built up of octahedra, are also observed in diphosphates $\text{CaM}_3(\text{P}_2\text{O}_7)_2$ ($M = \text{Co}, \text{Ni}$),²⁰ $\text{SrFe}_3(\text{P}_2\text{O}_7)_2$,²⁰ and $\text{PbM}_3(\text{P}_2\text{O}_7)_2$ ($M = \text{Fe}, \text{Co}, \text{Ni}$).^{21,22}

The projection of the structure along \vec{c} (Figure 4) shows that the P_2O_7 groups have their $\text{P}-\text{O}-\text{P}$ bond parallel to \vec{b} . Each P_2O_7 group ensures the connections between three $[\text{Cu}_3\text{O}_{10}]_\infty$ chains, forming with the latter four-sided tunnels running along \vec{c} . The P_2O_7 groups exhibit a practically eclipsed configuration and form small diamond shaped tunnels running along \vec{b} with the $[\text{Cu}_3\text{O}_{10}]_\infty$ chains.

Each diphosphate group consists of two independent tetrahedra, P(3) and P(4). Moreover the bond valence sum calculations (Table 3), according to Brown and Altermatt,²³ show that one valence is missing at the O(7) atom, belonging to the P(3) tetrahedra. Consequently the latter site is occupied by an OH group instead of an oxygen atom, so that the diphosphate groups are better formulated as $\text{P}_2\text{O}_6\text{OH}$ rather than P_2O_7 , leading for this diphosphate to the generic formula $\text{Cu}_3(\text{P}_2\text{O}_6\text{OH})_2$. The geometry of the P(3) and P(4) tetrahedra is similar to that usually observed for diphosphate groups. The $\text{P}-\text{O}$ bond that corresponds to the bridging oxygen O(8) is the longer in both tetrahedra (1.61–1.63 \AA), whereas the three other $\text{P}-\text{O}$ bonds are close to those observed in regular PO_4 tetrahedra, i.e., 1.51–1.53 \AA for P(4) and 1.51–1.59 \AA for P(3). Nevertheless the P(3) tetrahedron is slightly more distorted than the P(4) tetrahedron, due to the fact that it contains the OH group. The larger value of 1.59 \AA obtained for the $\text{P}-\text{OH}$ bond is in agreement with this statement. Note

(20) Lii, K. H.; Shih, P. F.; Chen, T. M. *Inorg. Chem.* **1993**, *32*, 4373.(21) Krasnikov, V. V.; Konstant, Z. A.; Bel'skii, V. K. *Izv. Akad. Nauk SSSR, Neorg. Mater.* **1985**, *21*, 1560.(22) Elmarzouki, A.; Boukhari, A.; Berrada, A.; Holt, E. M. *J. Solid State Chem.* **1995**, *118*, 202.(23) Brown, I. D.; Altermatt, D. *Acta Crystallogr. B* **1985**, *41*, 244.**Figure 3.** Structure of $\text{Cu}_3(\text{P}_2\text{O}_6\text{OH})_2$ viewed along the \vec{a} axis.**Figure 4.** Structure of $\text{Cu}_3(\text{P}_2\text{O}_6\text{OH})_2$ viewed along the \vec{c} axis.**Table 3.** Selected Distances and Calculated Valences for $\text{Cu}_3(\text{P}_2\text{O}_6\text{OH})_2$

	Cu1	Cu2	P3	P4	valence
O5		1.902(15)	1.512(13)		1.88
O6		1.982(16)		1.533(13)	2.14
		1.986(16)			
O7			1.592(15)		1.07
O8			1.611(20)	1.624(17)	2.00
O9	1.966(17) × 2			1.524(18)	1.75
O10	2.373(11) × 2	1.963(15)	1.512(14)		1.95
O11	1.991(13) × 2	2.333(13)		1.510(14)	1.94
valence	2.09	2.06	4.76	4.86	

also that in the $\text{P}_2\text{O}_6\text{OH}$ group, the P(3) tetrahedron exhibits one free corner corresponding to the OH group (O(7)), in contrast to the P(4) tetrahedron whose three other apexes are shared with copper polyhedra.

The tetragonal CuO_5 pyramids exhibit one longer apical $\text{Cu}-\text{O}$ bond (2.33 \AA) compared to distances in the basal plane, ranging from 1.90 to 1.99 \AA (Table 2). Such distances

in the basal plane evidence a rather strong distortion of the polyhedron. Such a feature is easily explained by the fact that each pyramid shares one edge with another pyramid, one edge with a CuO_6 octahedron, one edge with two apexes of the same $\text{P}_2\text{O}_6\text{OH}$ group, and two apexes with two different $\text{P}_2\text{O}_6\text{OH}$ groups, so that several of its apexes (O(10), O(11)) are tightly bonded to copper and phosphorus.

The CuO_6 octahedron is strongly elongated with two long apical Cu–O bonds of 2.37 Å, whereas in the basal plane, the Cu–O bonds, ranging from 1.97 to 1.99 Å (Table 2), show a much smaller distortion compared to CuO_5 pyramids. The smaller distortion of the CuO_6 octahedron may be due to the fact that it shares its six apexes with six different $\text{P}_2\text{O}_6\text{OH}$ groups, so that the strains are much smaller than for a pyramid for which one edge is shared with the same $\text{P}_2\text{O}_6\text{OH}$ group.

Although very different from the diphosphate $\text{Cu}_2\text{P}_2\text{O}_7$,¹¹ the structure of $\text{Cu}_3(\text{P}_2\text{O}_6\text{OH})_2$ exhibits some similarities. Both structures are indeed built up of copper chains interconnected by P_2O_7 groups. However the $[\text{CuO}_3]_\infty$ chains running along [110] and $[\bar{1}\bar{1}0]$ in this diphosphate consist of edge-sharing pyramids instead of pyramids and octahedra, and moreover each P_2O_7 group is never linked to the same pyramid but is shared between different pyramids.

Magnetic Properties. The inverse magnetic susceptibility of $\text{Cu}_3(\text{P}_2\text{O}_6\text{OH})_2$ (Figure 5) exhibits a Curie–Weiss behavior above 100 K. The data were least-squares fitted to a Curie–Weiss equation

$$\chi = \chi_0 + \frac{C}{T - \theta_p}$$

yielding $\theta_p = -32(2)$ K and an effective magnetic moment μ_{eff} per copper of $1.94 \mu_B$ was obtained. This value compares well to values commonly observed for Cu^{2+} (d^9) ions, while the negative paramagnetic temperature θ_p suggests an antiferromagnetic ordering transition at low temperature as observed in $\text{Cu}_2\text{P}_2\text{O}_7$ (Figure 5). Due to the one-dimensional nature of the copper chain, the low-temperature susceptibility may be analyzed using the numerical calculation for the 1D $S = 1/2$ system, given by the Bonner–Fisher expression:²⁴

$$\chi_{\text{chains}} = \frac{Ng^2\mu_B^2}{kT} \left[\frac{0.25 + 0.14995X + 0.30094X^2}{1 + 1.9862X + 0.68854X^2 + 6.0626X^3} \right]$$

where $X = |J|/kT$. With regard to the upturn of susceptibility below 40 K, a term was added, taking into account the Curie–Weiss susceptibility of monomeric impurities. The total susceptibility is then given by the following expression:

$$\chi_{\text{tot}} = \left\{ (1-x)\chi_{\text{chains}} + x \frac{Ng^2S(S+1)\mu_B^2}{3kT} \right\}$$

where x is the impurity fraction. The best fit of experimental data (continuous line on Figure 5) leads to $J = -21.9 \text{ cm}^{-1}$ ($J/k = -31.6\text{K}$), $g = 2.07$, and $x = 5.4\%$. Although these values appear reasonable, the poor fit of the experimental

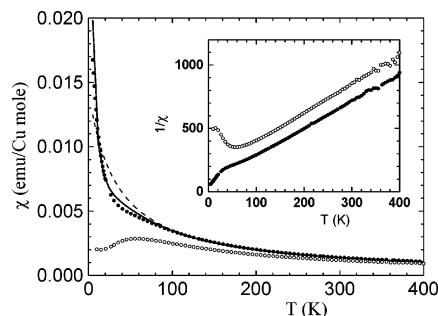


Figure 5. Magnetic susceptibility for $\text{Cu}_3(\text{P}_2\text{O}_6\text{OH})_2$ (filled circle) and $\text{Cu}_2\text{P}_2\text{O}_7$ (open circle). The susceptibility is given per mole of copper in order to compare the two compounds. The dashed line drawn through the data is a fit to the Curie–Weiss law between 100 and 400 K. The continuous line is a fit with the Bonner–Fisher expression for 1D $S = 1/2$ susceptibility. The inset shows the inverse susceptibility for the two compounds.

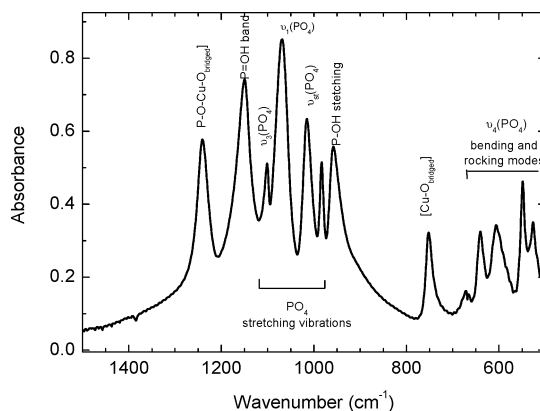


Figure 6. Infrared spectrum of the low wavenumber region of $\text{Cu}_3(\text{P}_2\text{O}_6\text{OH})_2$.

Table 4. Wavenumber Assignments for $\text{Cu}_3(\text{P}_2\text{O}_6\text{OH})_2$

wavenumber cm^{-1}	suggested assignments
1242	P–O–Cu deformation
1150	P–OH deformation
1100, 1068	$\nu_3(\text{PO}_4)$ antisymmetric stretching vibrations
1016, 984	$\nu_1(\text{PO}_4)$ symmetric stretching vibrations
955	P–OH stretching
751	Cu–O deformation modes
643, 603, 548, 525	$\nu_4(\text{PO}_4)$ out of plane bending vibration

susceptibility indicates that all of the fitted parameters should be considered with caution. Moreover the magnetic model of the susceptibility should contain two exchange integrals J_1 and J_2 in order to take into account magnetic interactions between $\text{Cu}(1)\text{–O–Cu}(2)$ and $\text{Cu}(2)\text{–O–Cu}(2)$.

Infrared Spectroscopy Study. The IR spectrum of the sample $\text{Cu}_3(\text{P}_2\text{O}_6\text{OH})_2$ is presented in Figure 6. The IR spectrum exhibits various absorption bands of lattice vibrations. The $\nu_{\text{st}}(\text{PO}_4)$ stretching bands appear in the range 960–1100 cm^{-1} (Table 4). These bands are split due to the distortion of the PO_4 tetrahedra in good agreement with the structural data. In addition, the 560–650 cm^{-1} region is assigned to out-of-plane bending modes of the phosphate ions. The hydroxide groups are observed at $\nu = 955$ and 1150 cm^{-1} (P–O–H band), and the bands due to the bonds Cu–O are located at 751 and 1242 cm^{-1} . These values are in a good agreement with the vibrational spectral analysis of pseudomalachite $\text{Cu}_5(\text{PO}_4)_2(\text{OH})_4$.²⁵

(24) Bonner, C. J.; Fisher, M. E. *Phys. Rev.* **1964**, *135*, A640.

Conclusion

A copper hydroxydiphosphate, $\text{Cu}_3(\text{P}_2\text{O}_6\text{OH})_2$, was synthesized by soft chemistry and structurally characterized. The structure is built up with zigzag chains of edge-sharing copper polyhedra linked by $\text{P}_2\text{O}_6\text{OH}$ groups. Its $[\text{Cu}_3\text{O}_{10}]_\infty$ chain consists of original trimers $\text{CuO}_5\text{—CuO}_6\text{—CuO}_5$ and looks like the zigzag chain observed in $\text{CaNi}_3(\text{P}_2\text{O}_7)_2$. Remarkably this compound is stable up to 400 °C, where dehydration occurs.

(25) Frost, R. L.; Kloprogge, T.; Williams, P. A.; Wayde Martens, W.; Johnson, T. E.; Leverett, P. *Spectrochim. Acta A* **2002**, *58*, 2861.

Acknowledgment. The authors gratefully acknowledge the European Union (Marie Curie Training Sites, Contract No. HPMT_CT_2000_00142), the Regional Council of Basse-Normandie, and the Ministry of Research for financial support.

Supporting Information Available: X-ray crystallographic file for $\text{Cu}_3(\text{P}_2\text{O}_6\text{OH})_2$ in CIF format. This material is available free of charge via the Internet at <http://pubs.acs.org>.

IC0485209